Direct Reversible Protein Electrochemistry at a Pyrolytic Graphite Electrode. Characterization of the Redox Thermodynamics of the Fe_4S_4-Siroheme Prosthetic Center in the Hexameric Dissimilatory Sulfite Reductase and the Monomeric Assimilatory Sulfite Reductase from *Desulfovibrio vulgaris* (Hildenborough). Systematic pH Titration Experiments and Implications for Active Site Chemistry[†,§]

Siu Man Lui and J. A. Cowan*[,‡]

Contribution from the Evans Laboratory of Chemistry, The Ohio State University, 120 West 18th Avenue, Columbus, Ohio 43210

Received June 7, 1994[⊗]

Abstract: Direct electrochemical studies have been performed on the dissimilatory hexameric sulfite reductase (DSiR, M_r ~200 000) and the assimilatory monomeric sulfite reductase (ASiR, M_r ~23 500) from *Desulfovibrio vulgaris* (Hildenborough). The reduction potential for the first redox couple of the $[Fe_4S_4]$-siroheme prosthetic center in DSiR has been determined as $E^{\circ\prime}$ (25 °C, pH 7.5) ~ −298 mV *versus* NHE by use of square-wave voltammetry with an edge pyrolytic graphite electrode (PGE) and redox inactive $Cr(NH_3)_6^{3+}$ promoter. The half-height peak width of 122 mV is in excellent agreement with the theoretical value of 126 mV expected for a reversible one-electron transfer with no coupled chemical reaction. Uptake of a second electron occurs at a reduction potential that is too negative to be detected over the range allowed while using the $Cr(NH_3)_6^{3+}$ redox promoter. The second reduction potential, $E^{\circ\prime}$ ~ −620 mV *versus* NHE was measured with a Hg(l) pool electrode by controlled potential coulometry (CPC). The reduction potentials for the first and second redox couples of the $[Fe_4S_4]$-siroheme prosthetic center in the assimilatory enzyme have been determined as $E_1^{\circ\prime}$ ~ −21 mV (siroheme) and $E_2^{\circ\prime}$ ~ −303 mV (cluster) *versus* NHE at pH 7.5 and 25 °C. The half-height peak width of 134 mV for the first redox couple (siroheme) is again in close agreement with the theoretical value of 126 mV expected for a reversible redox couple involving one-electron transfer; however, the half-height peak width for the second redox couple (Fe_4S_4 cluster) is only 84 mV. Diffusion controlled reversible heterogeneous electron transfer is observed for μM enzyme concentrations of either enzyme. For all signals observed in SWV the peak current (i_p) is proportional to the square-root of the frequency (ν) of the applied potential, indicative of diffusion control and rapid equilibrium conditions. The variation of peak current (i_p) with the amplitude of the square wave pulse (E_p) has also been examined. Enthalpic and entropic contributions to $E^{\circ\prime}$ values have been determined from variable temperature experiments as follows (pH 7.0 and 25 °C): DSiR, $\Delta H^{\circ\prime}$ −3.0 kcal mol^{-1}, $\Delta S^{\circ\prime}$ −31.3 eu; ASiR, $\Delta H^{\circ\prime}$ (siroheme) −11.8 kcal mol^{-1}, $\Delta S^{\circ\prime}$ (siroheme) −36.4 eu; $\Delta H^{\circ\prime}$ (cluster) −4.5 kcal mol^{-1}, $\Delta S^{\circ\prime}$ (cluster) −34.7 eu. Comparison is made with the redox thermodynamic parameters of cyt *c* (horse), myoglobin, and high potential iron protein. Systematic pH-titration studies provide evidence for coordination of an ionizable ligand to the prosthetic redox center, which is likely to be a bridging sulfide. For DSiR the electrochemical response for the first redox couple remains a single reversible peak over the entire pH range with a half-height peak width expected for one-electron exchange. The pH titration results support direct coupling of the siroheme and Fe_4S_4 cluster by the bridging ligand. The siroheme redox couple of ASiR shows an additional response in the pH titration curve (ascribed to an axial histidine residue) that is superimposed on the major broad pH-response from the enzyme. The detailed pH-dependence of both enthalpic and entropic parameters has been examined, and implications for active site chemistry are discussed. For DSiR, both ΔH° and ΔS° terms show no clear pH-dependence over the range from 3 to 10; however, for ASiR both the entropic and enthalpic components show a pH-dependence with an estimated pK_a^{ox} ~5.8 and pK_a^{red} of ~7.6. This is particularly pronounced for the siroheme redox couple and is proposed to originate from release of the axial histidine residue following reduction of the enzyme.

Introduction

Knowledge of the relative reduction potentials of redox prosthetic centers in metalloenzymes is an important factor in the evaluation of enzyme function and mechanism. Direct determination of reduction potentials has been demonstrated for redox active sites in low molecular weight electron-carrier proteins (5-20 kDa);[1-4] however, the methodology is not routine and requires extensive experimentation with solution

[†] Supported by the National Science Foundation (CHE-8921468).

[‡] J.A.C. is a Fellow of the Alfred P. Sloan Foundation, a Camille Dreyfus Teacher-Scholar, and a National Science Foundation Young Investigator.

[§] Abbreviations used: ASiR, assimilatory sulfite reductase; CPC, controlled potential coulometry; DEAE, diethylamino ethyl; DSiR, dissimilatory sulfite reductase; EDTA, ethylenediaminetetraacetic acid; EPR, electron paramagnetic resonance; $E^{\circ\prime}$, standard reduction potential; E_m, midpoint potential vs NHE; eu, entropy units (cal K^{-1} mol^{-1}); FPLC, fast protein liquid chromatography; K_a, association constant; M_r, molecular weight; PGE, pyrolytic graphite electrode; pI, isoelectric point; SWV, square wave voltammetry.

[⊗] Abstract published in *Advance ACS Abstracts*, November 1, 1994.

(1) Hill, H. A. O. *NATO ASI Ser., Ser. C* 1993; Vol. 385 (Molecular Electrochemistry of Inorganic, Bioinorganic and Organometallic Compounds), pp 133-49.

(2) Studies using membrane or matrix immobilization have also been reported. (a) Sucheta, A.; Cammack, R.; Weiner J.; Armstrong, F. A. *Biochemistry* **1993**, *32*, 5455. (b) Armstrong, F. A. *Struct. Bonding* **1990**, *72*, 137. (c) Sucheta, A.; Ackrell, B. A. C.; Cochran, B.; Armstrong, F. A. *Nature* **1992**, *356*, 362. (d) Heller, A. *Acc. Chem. Res.* **1990**, 23, 128. (e) Willner, I.; Katz, E.; Riklin, A.; Kasher, R. *J. Am. Chem. Soc.* **1992**, *114*, 10965.

0002-7863/94/1516-11538$04.50/0

conditions and electrode materials to obtain tractable data. EPR or optical methods of monitoring mediator titration experiments are more commonly used, although such techniques are of limited scope for studies that require systematic variation of solution pH or temperature. These potentiometric titration methods often suffer interference from the mediators employed, and so tedious background substraction is needed. In this paper we report the use of square-wave voltammmetry (SWV) with an edge pyrolytic graphite electrode (PGE) to perform direct electrochemistry on the 200 kDa dissimilatory sulfite reductase (DSiR) and the 23.5 kDa assimilatory sulfite reductase (ASiR) isolated from the sulfate reducing bacterium *Desulfovibrio vulgaris* (Hildenborough).[5-7] SWV enjoys several advantages over cyclic voltammetry and differential pulse voltammetry: including greater speed and sensitivity in analysis, lower consumption of electroactive species, and fewer problems arising from blockage of the electrode surface.[8-10] We have found this method to be very well suited to studies of many redox proteins and enzymes, requiring limited (μM) concentrations of sample.

Sulfite-reducing enzymes are generally thought to contain an active site containing an $[Fe_4S_4]$ cluster coupled to a siroheme by a bridge (Figure 1), either an inorganic S^{2-} bridge in the sulfite reductase from *Desulfovibrio vulgaris*[11-13] or possibly a cysteine bridge in the *E. coli* enzyme.[14-16] There is substantive evidence to support the direct coupling model for ASiR and *E. coli* sulfite reductase. Recently we have reported results that support this model for DSiR.[11,17] These two metalloredox centers serve as a catalytic apparatus for the enzymatic multi-electron reduction of SO_3^{2-} to S^{2-} and also NO_2^- to NH_3. Inasmuch as the reduction of SO_3^{2-} and NO_2^- anions to HS^- and NH_3, respectively, requires uptake of several proton equivalents (summarized in eqs 1 and 2), the mechanisms

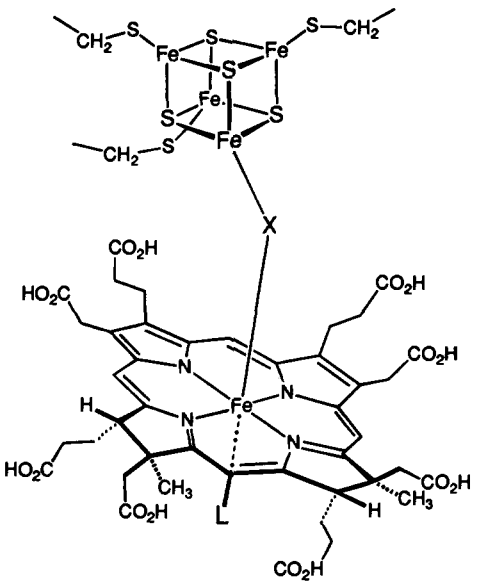

Figure 1. Schematic illustration of the prosthetic centers in assimilatory (ASiR, L = His, X = S^{2-}) and dissimilatory (DSiR, L = H_2O, or vacant, X = S^{2-}) sulfite reductase enzymes. The siroheme is low spin hexacoordinate for the former and high-spin pentacoordinate units for the latter. In each case the bridging ligand (X) is likely to be inorganic sulfide. Coupling has not been rigorously demonstrated for the dissimilatory enzyme by published data; however, our electrochemical data described herein and comparison with related systems, support such an assignment. Published variable temperature NMR data supports a coupled siroheme–cluster configuration for ASiR.[51]

utilized by the enzyme to promote efficient transfer of H^+

$$SO_3^{2-} + 6e^- + 7H^+ \rightarrow HS^- + 3H_2O \quad (1)$$

$$NO_2^- + 6e^- + 7H^+ \rightarrow NH_3 + 2H_2O \quad (2)$$

equivalents to the active site are clearly of importance. Since these proton transfer steps arise in the context of electron-transfer chemistry at the prosthetic center, it is reasonable to assume that the redox chemistry and proton transfer chemistry might be intimately coupled. The pH titration results reported herein demonstrate that electron uptake is indeed coupled to proton uptake and suggest that the dominant ionization site is the bridging ligand that connects the cluster and siroheme. The results of these experiments provide insight on active site chemistry and support direct coupling of the siroheme and $[Fe_4S_4]$ cluster to form a coupled redox pair (P) that apparently takes up two electrons in consecutive steps ($P \rightarrow P^- \rightarrow P^{2-}$).

In previous studies we have reported results from steady-state and pre-steady state kinetics measurements directed toward elucidation of mechanistic issues pertaining to this class of enzyme.[5,6] A rigorous understanding of the mechanism of sulfite reductase requires evaluation of the thermodynamic properties and pH-dependence of the two redox sites that constitute the prosthetic center. In turn, these offer insights on structural and bonding factors that control redox changes at the metal prosthetic centers. In this paper, we present a detailed characterization of the redox thermodynamics of these two enzymes and report the results of systematic pH titration experiments. The temperature dependence of the reduction potentials for the siroheme and cluster in ASiR and the first redox couple of DSiR have been monitored over a range of pH values, and key thermodynamic parameters have been evaluated. These thermodynamic constraints indicate some of the factors

(3) (a) Yeh, P.; Kuwana, T. *Chem. Lett.* **1977**, 1145. (b) Eddowes, M. J.; Hill, H. A. O. *J. Chem. Soc., Chem. Commun.* **1977**, 3154. (c) Armstrong, F. A.; Hill, H. A. O.; Oliver, B. N.; Walton, N. J. *J. Am. Chem. Soc.* **1984**, *106*, 921. (d) Butt, J. N.; Armstrong, F. A.; Breton, J.; George, S. J.; Thomson, A. J.; Hatchikian, E. C. *J. Am. Chem. Soc.* **1991**, *113*, 6663–6670. (e) Stankovich, M. T.; Bard, A. J. *J. Electroanal. Chem.* **1978**, *86*, 189–199. (f) Varfolomez, S. D., Berezen, I. V. *J. Mol. Catal.* **1978**, *4*, 387.

(4) Prior to our studies the largest example was a 115 kDa *p*-cresolmethylhydroxylase: Guo, L. H.; Hill, H. A. O.; Lawrence, G. A.; Sanghera, G. S.; Hopper, D. J. *J. Electroanal. Chem.* **1989**, *266*, 3379–396. Other studies on large proteins or protein–protein complexes by direct methods or immobilized systems include the following: Guo, L. H.; Hill, H. A. O.; Hopper, D. J.; Lawrance, G. A.; Sanghera, G. S. *J. Biol. Chem.* **1990**, *265*, 1958–63. Bagby, S.; Barker, P. D.; Guo, L. H.; Hill, H. A. O. *Biochemistry* **1990**, *29*, 3213–19. Sucheta, A.; Cammack, R.; Weiner J.; Armstrong, F. A. *Biochemistry* **1993**, *32*, 5455. Taniguchi, T. T.; Malmstrolm, B. G.; Anson, F. C.; Gray, H. B. *Proc. Natl. Acad. Sci. U.S.A.* **1982**, *79*, 3387.

(5) Lui, S. M.; Soriano, A.; Cowan, J. A. *J. Am. Chem. Soc.* **1993**, *115*, 10483–10486.

(6) Lui, S. M.; Liang, W.; Soriano, A.; Cowan, J. A. *J. Am. Chem. Soc.* **1994**, *116*, 4531–4536.

(7) Pierik, A. J.; Hagen, W. R. *Eur. J. Biochem.* **1991**, *195*, 505–516.

(8) (a) O'Dea, J. J.; Osteryoung, J. G.; Osteryoung, R. A. *Anal. Chem.* **1981**, *53*, 695. (b) Osteryoung, J. G.; Osteryoung, R. A. *Anal. Chem.* **1985**, *57*, 101A.

(9) (a) Smith, E. T.; Feinberg, B. A. *J. Biol. Chem.* **1990**, *265*, 14371–14376. (b) Ramaley, L.; Krause, M. S. *Anal. Chem.* **1969**, *41*, 1362.

(10) Smith, E. T.; Bennett, D. W.; Feinberg, B. A. *Anal. Chim. Acta* **1991**, *251*, 27–33.

(11) Wolfe, B. M.; Lui, S. M.; Cowan, J. A. *Eur. J. Biochem.* **1994**, *223*, 79–89.

(12) Huynh, B. H., Kang, L., DerVartanian, D. V., Peck, H. D., LeGall, J. *J. Biol. Chem.* **1984**, *259*, 15373–15376.

(13) Tan, J.; Cowan, J. A. *Biochemistry* **1991**, *30*, 8910–8917.

(14) McRee, D. E.; Richardson, D. C.; Richardson, J. S.; Siegel, L. M. *J. Biol. Chem.* **1986**, *261*, 10277–81.

(15) Cline, J. F.; Janick, P. A.; Siegel, L. M.; Hoffman, B. M. *Biochemistry* **1986**, *25*, 4647–4654.

(16) Madden, J. F.; Han, S.; Siegel, L. M.; Spiro, T. G. *Biochemistry* **1989**, *28*, 5471–5477.

(17) Lui, S. M.; Soriano, A.; Cowan J. A. *Biochem. J.* in press.

controlling redox changes at the prosthetic centers and also provide insight on mechanistic pathways.

Experimental Methods

General Materials. Buffer salts were of molecular biology grade (Fisher or Aldrich Chemical Co). Sephadex G-200 gel filtration material was obtained from Sigma and DEAE-52 ion exchange resin from Whatman. All water used was purified with a Barnstead nanopure system and exhibited a resistivity of 18 MΩ cm^{-1}. Chromium hexaammine trichloride was synthesized according to a literature procedure.[18] The Ag/AgCl reference electrode was purchased from BAS, and the Pt wire used as a counter electrode was purchased from Alfa. Pyrolytic graphite was obtained as a gift from Dr. R. L. McCreery at The Ohio State University.

Bacterial Growth. *Desulfovibrio vulgaris* (Hildenborough, NC1B 8303) was used as a source of DSiR, and *Desulfovibrio desulfuricans* G201 possessing a broad-host range expression vector (pDSK519) with the *D. vulgaris* ASiR gene and promoter cloned into the multiple cloning site provided ASiR.[19] Each was grown in a lactate-sulfate medium in 4 × 50 L carboys and harvested after 50 h growth at 32 °C using an Amicon DC 20 L concentrator. Small volumes of medium were deaerated by purging with Ar(g) (20 min) prior to inoculation. Larger volumes (50 L) were deaerated by purging with N_2(g) for 1 h prior to inoculation. Kanamycin (50 mg/L) was used as an antibiotic selector. Growth temperature (32−34 °C) was found to be critical to obtain the best yields of cell mass. About 450 g of cell paste were obtained from 200 L of culture solution and was stored at −80 °C prior to work up.

Enzyme Purification. The initial stages of isolation and purification of ASiR followed published procedures except for the final G-75 column, which was omitted.[11,12,20] DSiR was isolated and purified using procedures described elsewhere.[11] Enzyme samples were stable indefinitely if stored at −20 °C.

Direct Electrochemistry. ***Configuration of the Electrochemical Cell and Sample Preparation.*** A standard three-electrode configuration was used. Direct electrochemical measurements were performed with an edge pyrolytic graphite electrode (PGE) and redox inactive $Cr(NH_3)_6^{3+}$ as promoter. The PGE was made by embedding a strip of pyrolytic graphite with an exposed edge of surface dimensions 1 mm × 1 mm in an electrochemically-clean epoxy resin (Eccobond, Johnson-Matthey). A fresh PGE surface was cut for each experiment, followed by sonication in nanopure water to remove residual impurities. The reference electrode was a saturated Ag/AgCl electrode purchased from BAS. A length of platinium wire (4 cm × 1 mm) was used as the counterelectrode. The electrochemical cell was arranged in a nonisothermal configuration.[21−25] The reference electrode was held at constant temperature, while the temperature of the solution containing the redox-active material was set at an appropriate value. The electrochemical cell was double-walled with a water jacket that allowed the sample to be maintained at a constant temperature by a thermostatted circulating water bath. The temperature was recorded with an OMEGA HH 81 digital thermometer. All electrochemical experiments were performed with a positive pressure of O_2-free Ar(g) purging the surface of a 2 mL working solution. To prevent solvent loss over the course of several experiments, O_2-free Ar(g) was bubbled through degassed water to achieve water-saturation before purging the sample solution. No reduction in sample volume from evaporation was observed during the course of the experiment. The 2 mL volume of solution contained 8−10 μM enzyme with 8 mM $Cr(NH_3)_6^{3+}$ as promoter and 10 mM NaCl as supporting electrolyte in 10 mM potassium phosphate (buffered at the appropriate pH). The solution was purged with O_2-free, water-saturated Ar(g) for 15 min prior to running each experiment. Sample stirring was maintained during purging but not during data acquisition.

Electrochemical Data Acquisition and Analysis. Square wave voltammograms were obtained on a computer-interfaced PARC 263 potentiostat/galvanostat. Experimental conditions are noted in the figure legends. Before each voltammogram, the potential was routinely poised at 0 mV for 10 s to guard against the build-up of fouling products (which result in a greatly diminished response) at the electrode surface. After extensive experimental use (many scans) the electrode became aged and required reactivation by cutting a fresh surface. Following these procedures, voltammograms could be reproducibly obtained under the same experimental conditions. Reduction potentials were determined from the point at which the maximum net peak current was observed and are reported relative to the NHE. The number of electrons transferred per redox site were determined by measuring the observed peak width at half height ($W_{1/2}$). Under particular experimental conditions, the theoretically expected limiting value of $W_{1/2}$ for a reversible one-electron transfer by SWV, with no coupled chemical reaction, is 126 mV/n at 25 °C, where n is the number of electrons transferred.[26,27]

Controlled Potential Coulometry. ***Configuration of the Electrochemical Cell.*** The configuration of the electrochemical cell for the basic coulometric technique has been described by Watt and coworkers.[28,29] A three-electrode microelectrochemical cell of 60 μL capacity was made according to Smith and Adams.[30] The reference electrode is a saturated Ag/AgCl electrode purchased from BAS and the counterelectrode is a piece of Pt wire (4 cm × 1 mm) feathered and sealed in borosilicate tubing of 7 mm outer diameter. The working electrode is a Hg(l) pool of virgin grade purchased from Aldrich and further purified by filtering the mercury through a perforated filter paper (pinholed) to remove surface scum and oxides. Following Sawyer and Roberts, the mercury pool working electrode was constructed from a plastic support with a cup for a Hg pool at one end.[31] A carbon paste electrode (without carbon paste in the cup) was purchased from BAS to serve as the electrode support to hold the mercury pool. All three electrodes were equipped with an o-ring to form a tight seal with the cell body. The volume of the sample was kept to a minimum (a drop of 60 μL) so that complete electrolysis at each potential was achieved without the need for stirring. The three electrodes were immersed inside the drop of enzyme sample. The electrodes were separated by about 2 mm from each other. The set-up was analogous to the one employed by Su and Heineman who used a thin layer cell (OTTLE design) for coulometry measurements.[32] The relatively small distances between the electrodes minimizes IR drop. The set-up was successfully tested with methyl viologen, ferricyanide, and myoglobin, which yielded results (within experimental error) that were consistent with literature data.

Preparation of Samples for Coulometry. A 500 μL volume of enzyme solution of concentration 0.5 mM was stirred and purged with O_2-free Ar(g) in a 1 mL pear-shaped flask for 15 min. A second 1 mL pear-shaped flask containing a 500 μL volume of a mixed mediator solution was purged in a similar fashion. The mediators used were anthraquinone-2-sulfate ($E°_{NHE}$ = −225 mV); benzyl viologen dichloride ($E°_{NHE}$ = −440 mV); ethyl viologen ($E°_{NHE}$ = −480 mV); and

(18) Angelici, R. J. *Synthesis and Technique in Inorganic Chemistry*; University Science Books: Mill Valley, CA, 1986; pp 39−45.
(19) Tan, J.; Soriano, A.; Lui, S. M.; Cowan, J. A. *Arch. Biochem. Biophys.* **1994**, *312*, 516−523.
(20) Lee, J. P.; Le Gall, J.; Peck, H. D. *J. Bacteriol.* **1973**, *115*, 529−542.
(21) Taniguchi, V. T.; Ellis, W. R. Jr.; Cammarata, V.; Webb, J.; Anson, F. C.; Gray, H. B. In *Electrochemical and Spectrochemical Studies of Biological Redox Components*; Kadish, K. M., Ed.; American Chemical Society: Washington, D.C., 1982; p 51.
(22) Taniguchi, V. T.; Sailasuta-Scott, N. S.; Anson, F. C.; Gray, H. B. *Pure Appl. Chem.* **1980**, *52*, 2275−2282.
(23) Taniguchi, V. T.; Malmstrom, B. G. Anson, F. C.; Gray, H. B. *Proc. Natl. Acad. Sci.* U.S.A. **1982**, *79*, 3387.
(24) Reid, L. S.; Taniguchi, V. T.; Gray, H. B.; Mauk, A. G. *J. Am. Chem. Soc.* **1982**, *104*, 7516.
(25) Crutchley, R. J.; Ellis, W. R., Jr.; Gray, H. B. *J. Am. Chem. Soc.* **1985**, *107*, 5002.
(26) Smith, E. T.; Feinberg, B. A. *J. Biol. Chem.* **1990**, *256*, 14371−14376.
(27) Brumleve, T. R.; O'Dea, J. J.; Osteryoung, R. A.; Osteryoung J. *Anal. Chem.* **1981**, *53*, 702−706.
(28) Watt, G. D. *Anal. Biochem.* **1979**, *99*, 399−407.
(29) Watt, G. D.; Burns, A.; Lough, S.; Tennent, D. L. *Biochemistry* **1980**, *19*, 4926−4933.
(30) Smith, E. T.; Adams, M. W. W. *Anal. Biochem.* **1992**, *207*, 94−99.
(31) Sawyer, D. T.; Roberts, J. L., Jr. *Experimental Electrochemistry for Chemists*; John Wiley & Sons: New York, 1974; pp 79−86.
(32) Su, C.-H.; Heineman, W. R. *Anal. Chem.* **1981**, *53*, 594−598.

Scheme 1

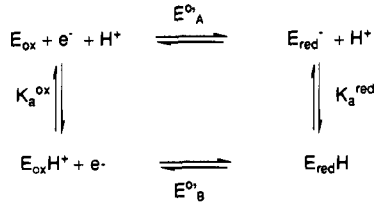

2-amino-4-pteridone ($E°_{NHE}$ = −660 mV).[33] Each mediator had a concentration of 0.5 mM in the final mixture. The three electrodes were screwed into the microelectrochemical cell with the o-rings inside swagelok fittings to provide a good seal and then flushed with O_2-free Ar(g) for 15 min, as were the experimental sample solutions. A gas-tight syringe (Hamilton) was flushed with O_2-free Ar(g) several times prior to withdrawing samples under a positive pressure of Ar(g). A 6 μL volume of mediator mixture and 54 μL of enzyme solution were withdrawn consecutively into a 100 μL gas tight syringe. The 60 μL sample solution was then injected into the preflushed microelectrochemical cell through a rubber septum. Care was taken to avoid displacing the Hg(l)-pool from the top of the working electrode. The rubber septum was then sealed with grease to prevent O_2 leakage. Final adjustment of the positions of the three electrodes was made at this point so that each electrode was immersed inside the sample drop and maintained at ~2 mm distance from each other to avoid direct contact. Argon purging was discontinued after adjusting the positions of electrodes. Final concentrations were 450 μM for the enzyme and 50 μM for the mediators (enzyme:mediator = 9:1). The buffer was 10 mM potassium phosphate solution at pH 7.5, containing 100 mM NaCl as supporting electrolyte. For each controlled potential coulometrical measurement, an identical control measurement was performed on a solution containing only mediators and buffer as a background reference. The corrected sample data for the enzyme solution was obtained by subtracting the background data from the raw sample data. For each measurement the potential was held until the current reached a small but constant level. The potential was then stepped to the next value and the procedure repeated. The time for each CPC measurement was kept at a constant value of 100 s.

Data Acquisition and Analysis. A controlled potential was supplied by a PAR 263 potentiostat equipped with a built-in electronic integrator. A modified headstart software from EG & G PARC was used to calculate the charge transferred at each potential. The potential was held until a complete decay curve was observed. The area under the decay curve was integrated to determine the charge transferred at that potential. A plot of number of electron equivalents transfered *versus* potential was obtained, and redox potentials were evaluated by fitting the data to eq 3,[34]

$$n = \left[\frac{1}{1 + 10^{(E - E_1)/0.059}}\right] + \left[\frac{1}{1 + 10^{(E - E_2)/0.059}}\right] \quad (3)$$

where n is the number of electrons taken up per half-molecule of DSiR (each molecule contains two [Fe_4S_4]–siroheme prosthetic centers) at a solution potential E, where E_1 and E_2 are the reduction potentials of the two redox couples in the prosthetic center of DSiR.

Variable Temperature Electrochemistry. A nonisothermal configuration was used for variable temperature electrochemical experiments. Weaver and co-workers have noted that the use of nonisothermal cells avoids certain problems associated with the reference electrodefor an isothermal cell configuration.[35] If the temperature coefficients of thermal junction potentials can be made either negligible or constant relative to the overall temperature coefficient of the nonisothermal cell (f(d$E°$,dT)), then this method provides a direct measure of the entropy change for half-cell reactions: $\Delta S°_{rc} = S°_{red} - S°_{ox} = nF(f(dE°,dT))$. When the magnitude of (f(d$E°$,dT)) is greater than 0.2 mV/deg,[36] errors arising from temperature gradients are small and can be neglected. The value of $\Delta S°_{cell}$ for the overall reaction was determined from the slope of a plot of potential versus temperature [$\Delta S°_{rc} = nF(f(d(\Delta E°),dT))$],[37] while the enthalpy change $\Delta H°$ was determined from the intercept.

Electrochemical pH Titration Experiments. Electron-exchange at protein-bound redox centers is frequently accompanied by ion (especially proton) uptake or release. Under such circumstances the reduction potential of the protein can be shown to vary with pH and can be quantitated by use of the Nernst equation.[40,41] The change in reduction potential with pH should follow a sigmoidal curve reflecting the pK_a^{ox} and pK_a^{red} of the ionizable residue or ligand near the redox center (Figures 11 and 12),[42] where the pK_a's are the equilibrium constants for the proton association of the ionizable ligand or residue for the oxidized and reduced forms of the protein (E). The equilibria are illustrated by Scheme 1,[22,26] which shows a thermodynamic cycle for the coupled electron- and proton-transfer reactions displaying a potentiometric behavior as shown in Figures 11 and 12. In our studies the pH data were fit by the standard eq 4, where E_m is the midpoint potential at different pH values, and $E°'$ is the standard

(33) (a) Spence, J. T.; Barber, M. J.; Siegel, L. M. *Biochemistry* **1982**, *21*, 1656–1661. (b) Kuwana, T. In *Electrochemical Studies of Biological Systems*; Sawyer, D. T., Ed.; ACS Symp. Series; Washington, DC, 1977; Vol. 38.

(34) Siegel, L. M.; Rueger, D. C.; Barber, M. J.; Krueger, R. J. *J. Biol. Chem.* **1982**, *257*, 6343–6350.

(35) Yee, E. L.; Cave, R. J.; Guyer, K. L.; Tyma, P. D.; Weaver, M. J. *J. Am. Chem. Soc.* **1979**, *101*, 1131.

(36) de Bethune, A. J.; Licht, T. S., Swendeman, N. *J. Electrochem. Soc.* **1959**, *106*, 606.

(37) The net entropy change for the complete cell reaction (referenced to NHE) is given by $\Delta S°_{cell} = \Delta S°_{rc} + (nS°_{H^+} - (n/2)S°_{H_2})$, where the $S°$ terms represent partial molal entropies. The entropy difference due to the reference electrode may be separated from that due to the redox couple of interest by use of the third law of thermodynamics.[38] The overall cell reaction entropy $\Delta S°_{cell}$ for a one-electron redox reaction can be written in the form of eq 6, when taking 31.2 eu for the partial molal entropy of H_2 and

$$\Delta S°_{cell} = \Delta S°_{rc} - 15.6 \text{ eu} \quad (6)$$

Latimer's convention of zero for $S°_{H^+}$.[39] Thus the entropy change for the overall cell reaction $\Delta S°_{cell}$ (determined from isothermal experiments) is equal to the reaction entropy $\Delta S°_{rc}$ (determined from nonisothermal experiment) after subtraction of 15.6 eu.

(38) Smith, E. B. *Basic Chemical Thermodynamics*; 2nd ed.; Oxford Chemistry Series: 1977.

(39) Latimer, W. M. *The Oxidation States of the Elements and Their Potentials in Aqueous Solutions*, 2nd ed.; Prentice-Hall: Englewood Cliffs, NJ, 1952.

(40) (a) Bard, A. J.; Faulkner, L. R. *Electrochemical Methods. Fundamentals and Applications*; Wiley: New York, 1980; pp 51–52. (b) p 143.

(41) For the redox reaction 7, which couples electron and proton transfer at 25 °C, the Nernst eq 8 can be rearranged to the form of eq 9. For most

$$E_{ox} + e^- + H^+ \rightleftharpoons E_{red}H \quad (7)$$

$$E = E° + (0.059)\log\left(\frac{[E_{ox}][H^+]}{[E_{red}H]}\right) \quad (8)$$

$$E = E° + (0.059)\log\left(\frac{[E_{ox}]}{[E_{red}H]}\right) - (0.059)\text{pH} \quad (9)$$

redox couples, proton transfer is limited by two pK_as: one for the oxidized form (pK_a^{ox}) and another at higher pH for the reduced form (pK_a^{red}). At intermediate pHs (pK_a^{ox} < pH < pK_a^{red}), proton uptake is coupled to the redox reaction. At solution pHs above and below the pK_a values, stoichiometric proton uptake no longer accompanies reduction. At pH ≫ pK_a^{red} the predominant redox reaction is defined by (10); however, at pH ≪ pK_a^{ox} the reaction is defined by (11).

$$E_{ox} + e^- \rightleftharpoons E_{red}^- \quad (10)$$

$$E_{ox}H^+ + e^- \rightleftharpoons E_{red}H \quad (11)$$

(42) Cowan, J. A. *Inorganic Biochemistry. An Introduction*; VCH: New York, 1993; p 88.

(43) Clark, W. M. *Oxidation-Reduction Potentials of Organic Systems*; Williams and Wilkins; Baltimore, MD; 1960.

reduction potential.[43]

$$E_m = E^{\circ\prime}{}_B - 59\log\left(\frac{K_a^{red}(1 + K_a^{ox}[H^+])}{K_a^{ox}(1 + K_a^{red}[H^+])}\right)\text{mV} \quad (4)$$

Results

Determination of Reduction Potentials. ***Assimilatory Sulfite Reductase (ASiR).*** With the high sensitivity of SWV, we were able to obtain an electrode response from a microedge PGE (1 mm × 1 mm) at μM concentrations of enzyme. Typically a scan range from 0 to −600 mV *versus* NHE was used. The square wave conditions used in specific experiments are noted in the figure legends. Repulsive interactions between oxygen-containing functional groups on the graphite surface and acidic residues on ASiR (pI ~ 4.6) were electrostatically neutralized by adding high valent $Cr(NH_3)_6^{3+}$ as a promoter.[44,45] Two discrete electron-transfer steps were readily seen in direct electrochemical measurements (Figure 2) at an edge PGE with $Cr(NH_3)_6^{3+}$ as a redox promoter. Previous EPR (Figure 3, top) and optical data had suggested that the enzyme undergoes two discrete reduction steps, with the first electron adding to the siroheme followed by the addition of a second electron equivalent to the cluster.[46] The reduction potentials for the siroheme and cluster were determined to be −21 and −303 mV, respectively, *versus* NHE at pH 7.5, 25 °C. The more positive peak was assigned to the siroheme redox couple on the basis of EPR results for partially reduced enzyme.[46]

Dissimilatory Sulfite Reductase (DSiR). Similarly, the reduction potential for the first redox couple of the $[Fe_4S_4]$–siroheme prosthetic center has been determined to be $E^{\circ\prime}$ (25 °C, pH 7.5) ~ −298 mV *versus* NHE and corresponds to one-electron transfer to the redox site (Figure 4). At higher pH, increased concentrations of $Cr(NH_3)_6^{3+}$ were required to obtain an electrode response from DSiR (2 mM at pH 3.0 *versus* 8 mM at pH 8.5). Presumably there is more extensive electrostatic repulsion as a result of deprotonation of additional functional groups on both the enzyme and the electrode. Similar observations were made with experiments on ASiR.

The difference in reduction potentials between siroheme and cluster in ASiR was measured to be 280 mV by the SWV method. In contrast, only one peak at −298 mV was obtained for DSiR in the SWV scan from +200 mV to −500 mV *versus* NHE (Figure 4). Scans to more negative potentials (up to −800 mV) were attempted, but no second peak was observed. Uptake of a second electron occurs at a reduction potential that is too negative to be detected in the presence of the $Cr(NH_3)_6^{3+}$ promoter, which is reduced,[45] and so controlled potential coulometry (CPC) was performed to obtain the second reduction potential for DSiR. The coulometry data was obtained with a Hg(l)-pool working electrode. Two potentials were detected at ~ −320 and −620 mV *versus* NHE (Figure 5). The data was corrected by substracting the background data from raw data. Within experimental error, the first redox potential (−298 mV) obtained from SWV shows good general agreement with the potential of −320 mV determined by the CPC method. The difference in reduction potentials between the first and second redox couples was estimated to be 300 mV by the CPC method. Table 1 summarizes the redox potentials for ASiR and DSiR from *D. vulgaris* and for comparison also lists data for the assimilatory sulfite reductase from *E. coli*, cytochrome *c*, myoglobin, and hemoglobin.

Previous EPR studies (Figure 3, top) on photoreduced intermediates of DSiR have suggested that the $[Fe_4S_4]$ cluster and siroheme have similar reduction potentials and that a single electron is shared by the siroheme and $[Fe_4S_4]$ cluster.[17] That is, the oxidized siroheme EPR signal decreases by half with the appearance of half of the reduced cluster signal. At any stage in the photoreduction the ratio of siroheme-to-cluster signals was found to be similar when the reduction was carried out either in the absence or presence of a mediator system, within the error limits resulting from background mediator signals, and so these spectra represent true thermodynamic equilibria. Upon one-electron reduction of DSiR, approximately one-half of the molecules contain reduced siroheme and the other half contain reduced cluster (Figure 6B). This behavior contrasts with the two distinct potentials (for siroheme and cluster) found for the assimilatory sulfite reductase enzymes from *D. vulgaris* (Figure 6A) and *E. coli*. We postulate that the siroheme and cluster in DSiR form a bridged redox pair that apparently takes up two electrons in consecutive steps ($P \rightarrow P^- \rightarrow P^{2-}$).

Evidence for Direct Reversible Electrochemistry. In a reversible redox process, the concentration of species at the electrode surface depends only on thermodynamic considerations; that is, according to the equilibrium established by the applied potential at the electrode surface. The current-time response under the appropriate applied potential then follows the Cottrell eq 5, where n is the number of electrons

$$i = \frac{nFAD^{1/2}C^*}{\pi^{1/2}t^{1/2}} \quad (5)$$

transferred/redox site/molecule, F is the Faraday constant, A is the cross-sectional area normal to the axis of mass flow, D is the diffusion coefficient of the redox species, and C^* is the bulk concentration of the redox species. When applying the Cottrell equation to SWV, a plot of i_p *versus* $v^{1/2}$ is linear if diffusion control and rapid equilibrium conditions exist, and so such a plot provides an indication of the extent to which the electrode kinetics influences the equilibrium at the electrode.[40b] In Figures 2 and 4 (middle) it is shown that the peak current i_p is directly proportional to the square-root of the frequency of the applied potential for each of the signals observed by the SWV method; that is, the reduction potentials determined for the siroheme and cluster couples in ASiR and the first redox couple in DSiR. The linearity of the plots of i_p *versus* $v^{1/2}$ for the aforementioned data sets indicates that the current is diffusion controlled for each of these redox couples, suggesting that direct electron transfer between the electrode and the sulfite reductase enzymes from *D. vulgaris* was indeed taking place and that diffusion control and rapid equilibrium conditions existed during the electrochemical measurement.

The dependence of current density $[i/(n^*W_{1/2})]$ on square-wave amplitude (Figures 2 and 4, lower) also shows excellent agreement with theoretical expectations,[8a] where n is the number of electron equivalents estimated for each of the responses as described above. The current density increases but then levels off to a maximum since increased amplitudes lead to broadening of the observed current peak.[8a,47]

Nernstian *n*. Theoretically, the limiting value of the peak width at half-height ($W_{1/2}$) in SWV is $126/n$ mV for a reversible one-electron transfer with no coupled chemical

(44) Armstrong, F. A.; Bond, A. M.; Hill, H. A. O.; Oliver, B. N.; Psalti, I. S. M. *J. Am. Chem. Soc.* **1989**, *111*, 9185.

(45) Armstrong, F. A.; Cox, P. A.; Hill, H. A. O.; Lowe, V. J.; Oliver, B. N. *J. Electroanal. Chem.* **1987**, *217*, 331–366.

(46) Lui, S. M.; Cowan, J. A., manuscript in preparation.

(47) Christie, J. H.; Turner, J. A.; Osteryoung, R. A. *Anal. Chem.* **1977**, *49*, 1899.

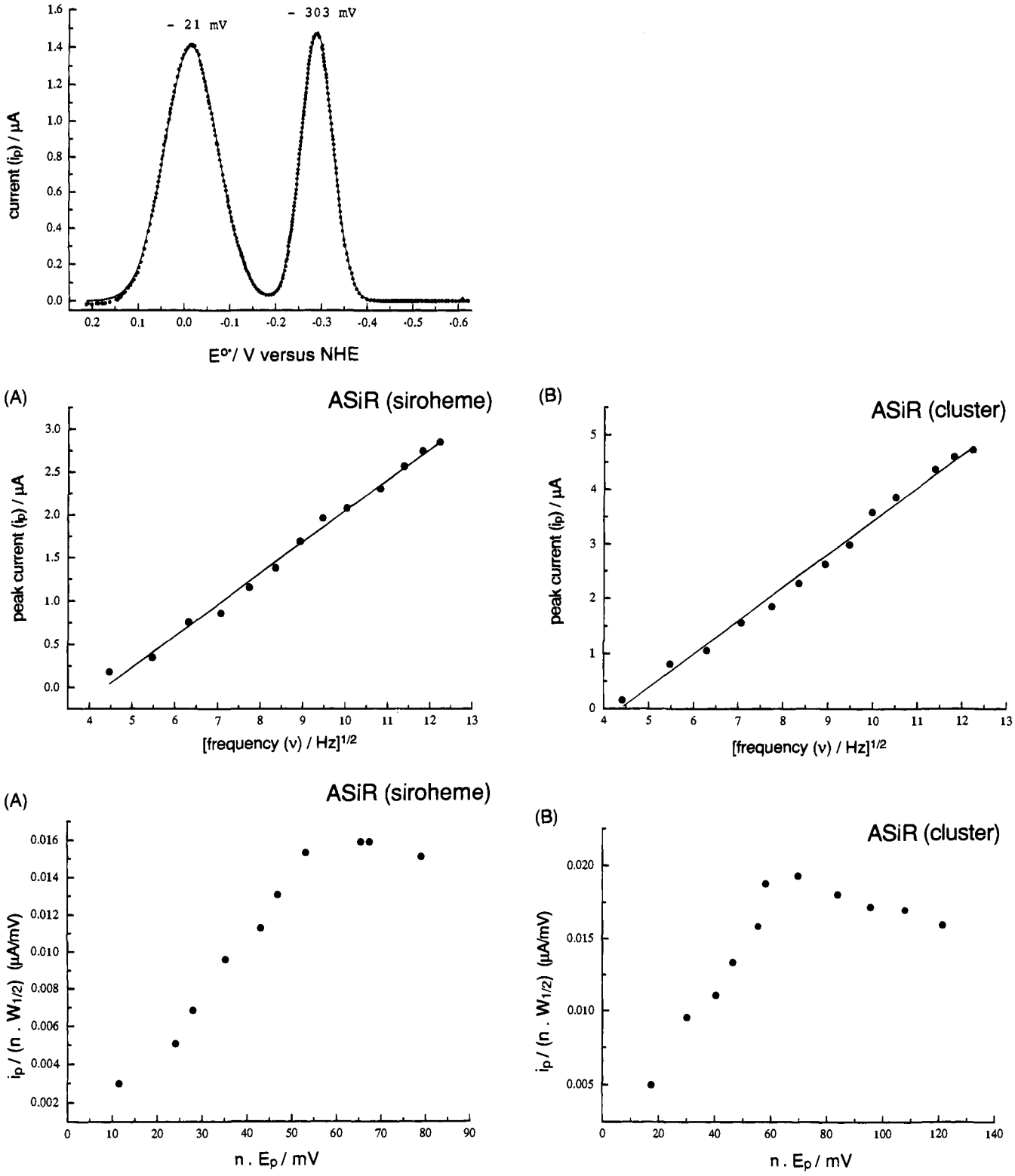

Figure 2. (Top) A typical square wave voltammogram obtained from an 8 μM ASiR solution with 8 mM $Cr(NH_3)_6^{3+}$ in 10 mM potassium phosphate/ 10 mM NaCl under Ar(g) (298 K, pH 7.5). SWV conditions: pulse potential (E_p) = 50 mV; step potential (E_s) = 1 mV; frequency of the applied potential = 140 Hz. The solid line shows a Gaussian fit of the data. (Middle) Dependence of the peak current (i_p) on the square root of the frequency of the applied potential pulse ($\nu^{1/2}$) for the siroheme (A) and cluster (B) redox couples. (Bottom) Dependence of the peak current density ($i_p/nW_{1/2}$) on the amplitude of the square wave pulse (nE_p) for the siroheme (A) and cluster (B) redox couples.

reaction, depending on the square-wave parameters employed.[26] For ASiR, the magnitude of $W_{1/2}$ was found to be 134 mV for the siroheme signal and 84 mV for the cluster signal, equivalent to a value of 0.94 electrons transferred at the siroheme site and 1.5 electron equivalents transferred at the cluster site. This slightly larger than expected value for the cluster signal most likely reflects the oxidative instability of this highly reduced form and may reflect a coupled side-reaction with H_2O or trace O_2. For DSiR, the $W_{1/2}$ value for the first redox couple was 122 mV (corresponding to the transfer of 1.03 electron equivalents); again in excellent agreement with the theoretical value expected for a reversible redox couple involving one-electron

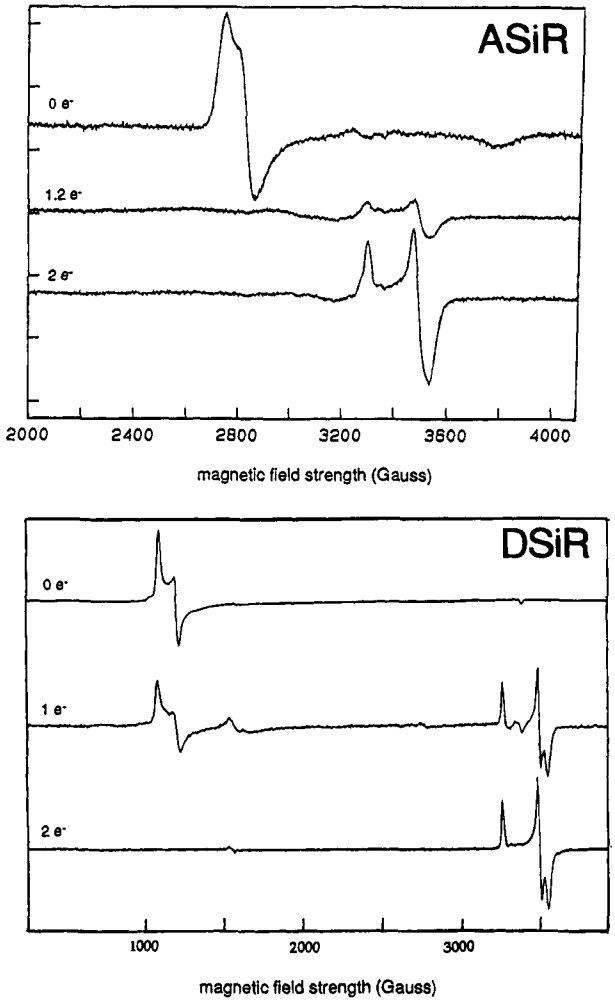

Figure 3. (Top) Stacked EPR spectra of ASiR with 0, 1.2, and 2 electron equivalents added per siroheme/cluster couple showing the disappearance of oxidized siroheme after addition of one-electron equivalent and prior to the appearance of the reduced cluster. (Bottom) Stacked EPR spectra of DSiR with 0, 1, and 2 electron equivalents added per siroheme/cluster couple showing the simultaneous appearance of oxidized siroheme and reduced cluster of desulfoviridin after addition of one-electron equivalent. Ratios of siroheme-to-cluster signals were found to be similar when the reduction was carried out either in the absence or presence of a mediator system. Adapted from refs 17 and 46 for comparison with electrochemical data.

transfer. From the controlled potential coulometrical measurements made on DSiR, the number of electron equivalents transferred (n) was estimated to be 0.94 and 0.89 for the first and second redox couples ($P \rightarrow P^-$ and $P^- \rightarrow P^{2-}$), respectively.

Determination of Enthalpic and Entropic Components. The temperature dependence of the first reduction potential of DSiR and the two reduction potentials of ASiR are illustrated in Figures 7 and 8. The solid line is a linear least-squares fit to the data, and the redox thermodynamic parameters derived from these nonisothermal experiments are summarized in Table 2. It is significant that the $\Delta S^{\circ\prime}$ values are all negative and are large in magnitude in comparison with related data obtained from horse cytochrome c (a low-spin heme, $\Delta S^{\circ\prime} = -28.5$ eu)[21,23] but smaller than the high-spin heme in myoglobin ($\Delta S^{\circ\prime} = -38$ eu).[25] Interestingly, the $\Delta S^{\circ\prime}$ value for low-spin ASiR shows more similarity to the value reported for high-spin Mb, while the $\Delta S^{\circ\prime}$ value for high-spin DSiR shows more similarity to the value reported for low-spin cytochrome c. There seems to be no obvious relationship between the spin state and the magnitude of $\Delta S^{\circ\prime}$ values. The significance of these findings

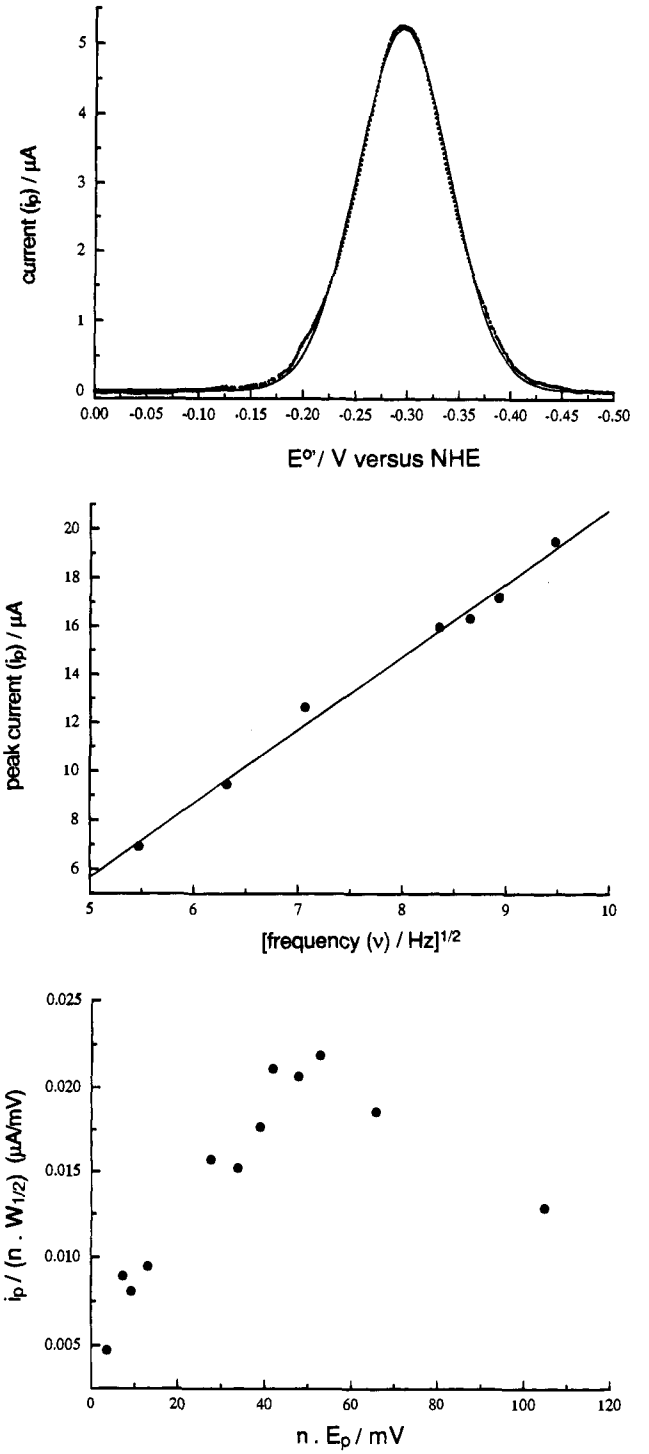

Figure 4. (Top) A typical square wave voltammogram obtained from a 10 μM DSiR solution with 8 mM $Cr(NH_3)_6^{3+}$ in 10 mM potassium phosphate/10 mM NaCl (298 K, pH 7.5) under Ar(g). SWV conditions: pulse potential = 50 mV; step potential = 1 mV; frequency of the applied potential = 100 Hz. The solid line shows a Gaussian fit of the data. The peak width at half-height is 122 mV, in excellent agreement with the theoretical value of 126 mV expected for a reversible redox couple involving one-electron transfer. (Middle) For each response the peak current (i_p) is proportional to $\nu^{1/2}$, where ν is the frequency of the applied potential. This indicates that the electroactive species is under diffusion control and that the enzyme interacts reversibly with the electrode surface. (Bottom) Dependence of the peak current density ($i_p/nW_{1/2}$) on the amplitude of the square wave pulse (nE_p).

for an understanding of active site chemistry is a topic of discussion later in the text. It is also noteworthy that the $\Delta H^{\circ\prime}$

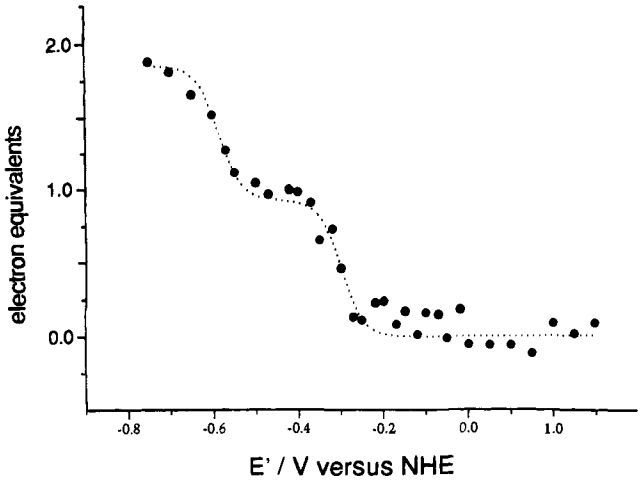

Figure 5. Controlled potential coulometry data showing the total number of electron equivalents taken up by the cluster/siroheme couple in DSiR at an applied potential E'. For each data set a background data set was taken in the absence of enzyme. Final concentrations were 450 μM for the enzyme and 50 μM for the mediators. The buffer was 10 mM potassium phosphate solution at pH 7.5, containing 100 mM NaCl as supporting electrolyte. The time for each CPC measurement was kept at a constant value of 100 s. The plotted data was fit to eq 3.

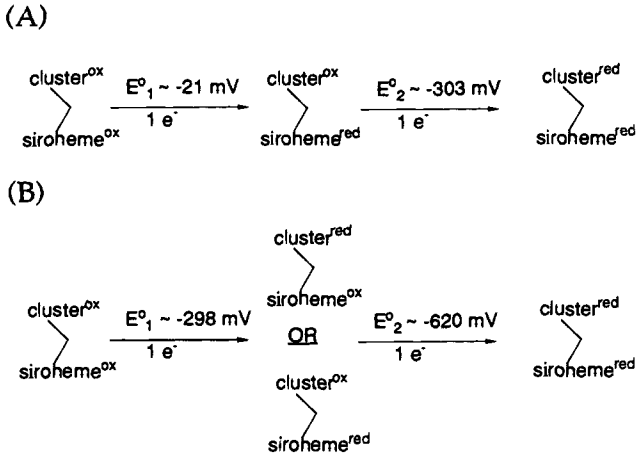

Figure 6. Summary of enzyme electrochemistry: (A) ASiR and (B) DSiR.

value for the siroheme in ASiR (−11.8 kcal mol^{-1}) is significantly more negative in comparison to $\Delta H^{\circ\prime}$ values for the cluster in ASiR and the first redox couple in DSiR (−4.5 and −3.0 kcal mol^{-1}, respectively) but shows more similarity to the $\Delta H^{\circ\prime}$ values for cyt *c* and Mb (−14.5 and −14.0 kcal mol^{-1}). The $\Delta H^{\circ\prime}$ values for the redox couples listed in Table 2 are all negative in magnitude. The more negative $\Delta H^{\circ\prime}$ for ASiR siroheme, cyt *c*, and Mb most likely reflects favorable metal to ligand d-π orbital overlap with an axial histidine residue, which tends to stabilize the ferrous ion in the porphyrin or sirohydrochlorin ligand.

pH-Dependence of Enthalpic and Entropic Components. Figure 9A shows the sigmoidal pH-dependence of ΔS° observed for the siroheme signal in ASiR, with a half-midpoint change for ΔS° suggesting a neighboring ionizable site with a pK_a ~ 6.9. This type of response was observed only weakly for the cluster signal in ASiR (Figure 9C), while the first redox couple (P → P$^-$) in DSiR showed essentially no pH-dependence for ΔS° (Figure 10A).

The pH-dependence of the enthalpic components (ΔH°) essentially followed similar trends to those described for the entropic terms. The siroheme response in ASiR demonstrated

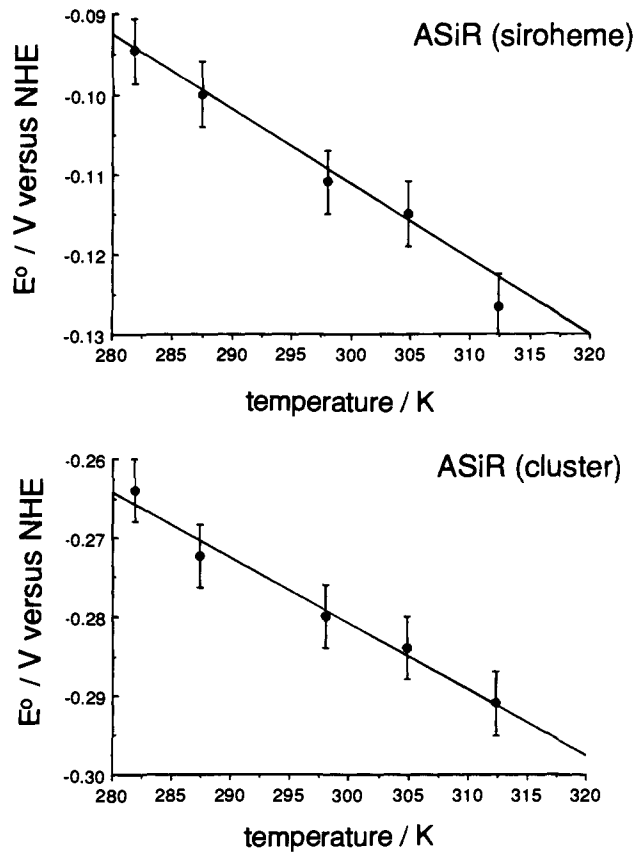

Figure 7. Temperature dependence of the reduction potential of the siroheme–cluster redox couples in ASiR (pH 7.0): (top) siroheme and (bottom) cluster. The entropic (ΔS°) and enthalpic (ΔH°) terms were determined from the slope and intercept of an E° versus T plot.

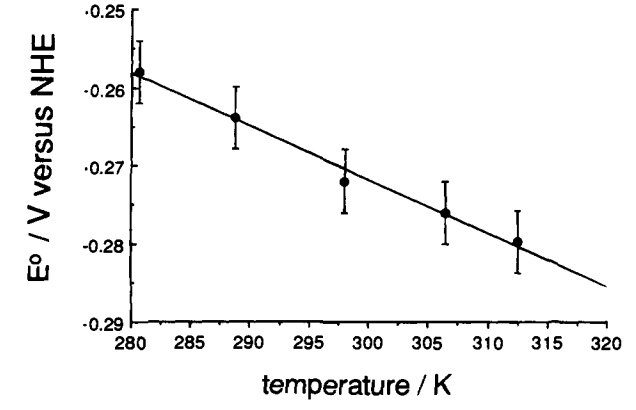

Figure 8. Temperature dependence of the first reduction potential of the siroheme–cluster redox couple in DSiR (pH 7.0). In DSiR, the first reduction potential includes contributions from both the siroheme and [Fe_4S_4] cluster. See the legend to Figure 7 for further elaboration on the format of this figure.

a weak but noticeable dependence on pH (pK_a ~ 6.7, Figure 9B); however, neither the cluster response from ASiR nor the first reduction response from DSiR demonstrated any systematic pH-dependence over background error (Figures 9D and 10B, respectively).

pH-Dependence of Reduction Potentials. The pH-dependence of E° for ASiR and DSiR were examined at 25 °C (Figures 11 and 12, respectively), and the gradients ($\Delta E^\circ/\Delta$pH) from the central region of the plots were determined as follows: ASiR siroheme, ΔE° = −64 mV/pH unit; ASiR cluster, ΔE° = −56 mV/pH unit; DSiR, ΔE° = −62 mV/pH unit. We estimate an e$^-$/H$^+$ transfer ratio of approximately one

Table 1. $E^{\circ\prime}$ Values for the Redox Couples in ASiR and DSiR from *D. vulgaris* Using SWV and CPC Methods

enzyme	redox site	$E^{\circ\prime}$ (mV) *vs* NHE	ref
ASiR (25 °C, pH 7.5)[a]	siroheme	−21	this work
	cluster	−303	this work
DSiR (25 °C, pH 7.5)[b]	1st redox couple (P^-)	−298	this work
	2nd redox couple (P^{2-})	−620	this work
E. coli sulfite reductase[a,c]	siroheme	−340	54b
	siroheme-CN^-	−155	55
	cluster-CN^-	~ −490	55
cyt *c* (horse)	heme	+250	49
myoglobin	heme	+50	49
hemoglobin	heme	+170	49

[a] For ASiR and *E. coli* sulfite reductase, $E_1^{\circ\prime}$ represents the reduction potential for the siroheme, while $E_2^{\circ\prime}$ represents the reduction potential for the [Fe_4S_4] cluster. [b] For DSiR, $E_1^{\circ\prime}$ represents the reduction potential for the first redox couple. $E_2^{\circ\prime}$ has not been determined by direct electrochemistry but has been estimated as ~ −620 mV by controlled potential coulometry. [c] For *E. coli* sulfite reductase the potentials were estimated by EPR mediator titrant techniques. For native enzyme, the relative difference of 65 mV reported for the cluster and siroheme potentials is distinct and different from the absolute potentials for reduction of the combined redox center in the enzyme by one- and two-electron equivalents. Refer to Figure 6B and ref 17 for further clarification on this point.

Table 2. Redox Thermodynamic Parameters at pH 7.0 and 25 °C

	$\Delta S^{\circ\prime}_{cell}$ (eu)	$\Delta S^{\circ\prime}_{rc}$ (eu)	$\Delta H^{\circ\prime}$ (kcal mol^{-1})	$\Delta G^{\circ\prime}$ (kcal mol^{-1})	$E^{\circ\prime}$ (V) vs NHE	ref
ASiR						
siroheme	−36.4	−20.8	−11.8	+0.97	−0.042	this work
cluster	−34.7	−19.1	−4.5	+5.8	−0.251	this work
DSiR						
1st redox couple (P^-)	−31.3	−15.7	−3.0	+6.3	−0.272	this work
cyt *c* (horse)	−28.5	−12.9	−14.5	−6.0	+0.260	21, 22
Mb	−38.0	−22.4	−14.0	−2.8	+0.120	25
HiPIP	−25.6	−10.0	−15.8	−8.1	+0.350	21, 22

Table 3. pK_a^{ox} and pK_a^{red} Values Obtained from pH Titration Studies at 25 °C for ASiR and DSiR Using SWV Methods[a]

enzyme	redox couple	pK_a^{ox}	pK_a^{red}
ASiR	siroheme	3.7	9.9
	cluster	3.8	9.9
DSiR	1st redox couple (P^-)	3.2	9.0

[a] Experimental conditions were the same as in the legend to Figure 11 for ASiR and Figure 12 for DSiR.

for each redox couple observed. The pH data were fit by the standard eq 4 to yield two pK_a values (pK_a^{ox} and pK_a^{red}) that are summarized in Table 3. The separation of ($pK_a^{red} - pK_a^{ox}$) ~ 6 units is large in comparison to the difference typically obtained for ionizable residues neighboring a redox site; however, such a separation has previously been observed for met-Mb which possesses a bound water molecule.[48] It is possible, therefore, that the response obtained derives from either a siroheme-bound H_2O or a bridging sulfide ligand. Clearly redox chemistry at the prosthetic site is intrinsically coupled to an influx of protons and is most likely of functional significance given the fact that sulfite or nitrite reduction requires uptake of at least seven proton equivalents. One-electron exchange is also supported by analysis of the signal response (Figures 2 and 3). The peak width at half-height for the electrode response is generally in excellent agreement with the theoretical value of 126 mV expected for a reversible redox couple involving one-electron transfer.[26]

Discussion

Comparison of Reduction Potentials for ASiR and DSiR. Table 1 summarizes the electrochemically-determined reduction potentials for the redox couples in the prosthetic centers of ASiR and DSiR from *D. vulgaris* and makes the comparison with published data on the *E. coli* assimilatory sulfite reductase and other common heme proteins. The siroheme and [Fe_4S_4] cluster form a coupled redox pair (P) (shown in Figure 1) that apparently takes up two electrons in consecutive steps ($P \rightarrow P^- \rightarrow P^{2-}$). In the case of ASiR the sequence of electron additions is to siroheme first with subsequent reduction of the cluster (Figure 3, top). In contrast, the relative potentials of the siroheme and cluster in DSiR appear to be similar (Figure 6), and each electron added can be best regarded as shared between the siroheme and cluster. Both enzymes can be readily photoreduced in the solution state in an ice water bath.[17,46] At liquid helium temperatures, electron exchange for the one-electron reduced center is apparently frozen out, and individual features from the reduced cluster center and oxidized siroheme can be observed by EPR techniques (Figure 3, bottom).

The reduction potentials of each of the first redox couples of [Fe_4S_4]−siroheme prosthetic centers lie in the negative range of $E^{\circ\prime}$ values, while the hemes in myoglobin, cyt *c*, and hemoglobin have positive $E^{\circ\prime}$ values (+50, +250, and +170 mV, respectively).[49] The principal feature that distinguishes the two classes of heme center in these enzymes (siroheme and heme) lies in the degree of saturation of the porphyrin-derived macrocycle. In the former case the elements of methane (CH_4) have been added across two pyrrolic rings (Figure 1). The additional electron density on the siroheme ring tends to stabilize the Fe(III) state, resulting in more negative $E^{\circ\prime}$ values in comparison to the heme in Mb, Hb, and cyt *c*. This is also reflected by the ease of oxidation of the siroheme ring, which in some circumstances may be more facile than oxidation of the ferrous ion in reduced siroheme.[50a] It should be noted, however, that other proteins carrying standard hemes do show negative potentials (for example, cytochrome P-450s and catalase), and so the reduced ring is not a prerequisite for a negative reduction potential.[50] Clearly, in certain cases the protein environment can play a dominant role in poising reduction potentials.

It was noted that the first redox couple in ASiR (corresponding to siroheme reduction) has a less negative $E^{\circ\prime}$ value in comparison to DSiR and *E. coli* sulfite reductase. This may well arise from the presence of a sixth ligand (proposed as His)[51] that can stabilize the reduced form of siroheme, giving rise to a more positive potential. Both DSiR and *E. coli* sulfite reductase contain high-spin pentacoordinate siroheme. Alternatively, the increase in the $E^{\circ\prime}$ value for siroheme in ASiR

(48) Antonini, E.; Brunori, M. *Frontiers of Biology. Hemoglobin and Myoglobin*; North-Holland Publishing Co.: Amsterdam, 1971; Vol. 21, pp 327−347.

(49) Moore, G. R.; Williams, R. J. P. *Coordination Chem. Rev.* **1976**, *18*, 125−197.

(50) The general trend of increasingly negative reduction potentials for the more saturated ring systems is followed fairly rigorously when comparing data for model metallo-porphyrin chromophores with similar axial ligands [refs (a) and (b), below]. This tends to support a strong influence by the protein environment in defining reduction potentials for certain metalloredox proteins or enzymes: (a) Chang, C. K.; Hanson, L. K.; Richardson, P. F.; Young, R.; Fajer, J. *Proc. Natl. Acad. Sci. U.S.A.* **1981**, *78*, 2652−2656. (b) Kadish, K. In *Iron Porphyrins*; part 2, Physical Bioinorganic Chemistry Series, Lever, A. B. P., Gray, H. B., Eds.; Addison-Wesley: New York, 1983.

(51) Cowan, J. A.; Sola, M. *Inorganic Chem.* **1990**, *29*, 2176−2179.

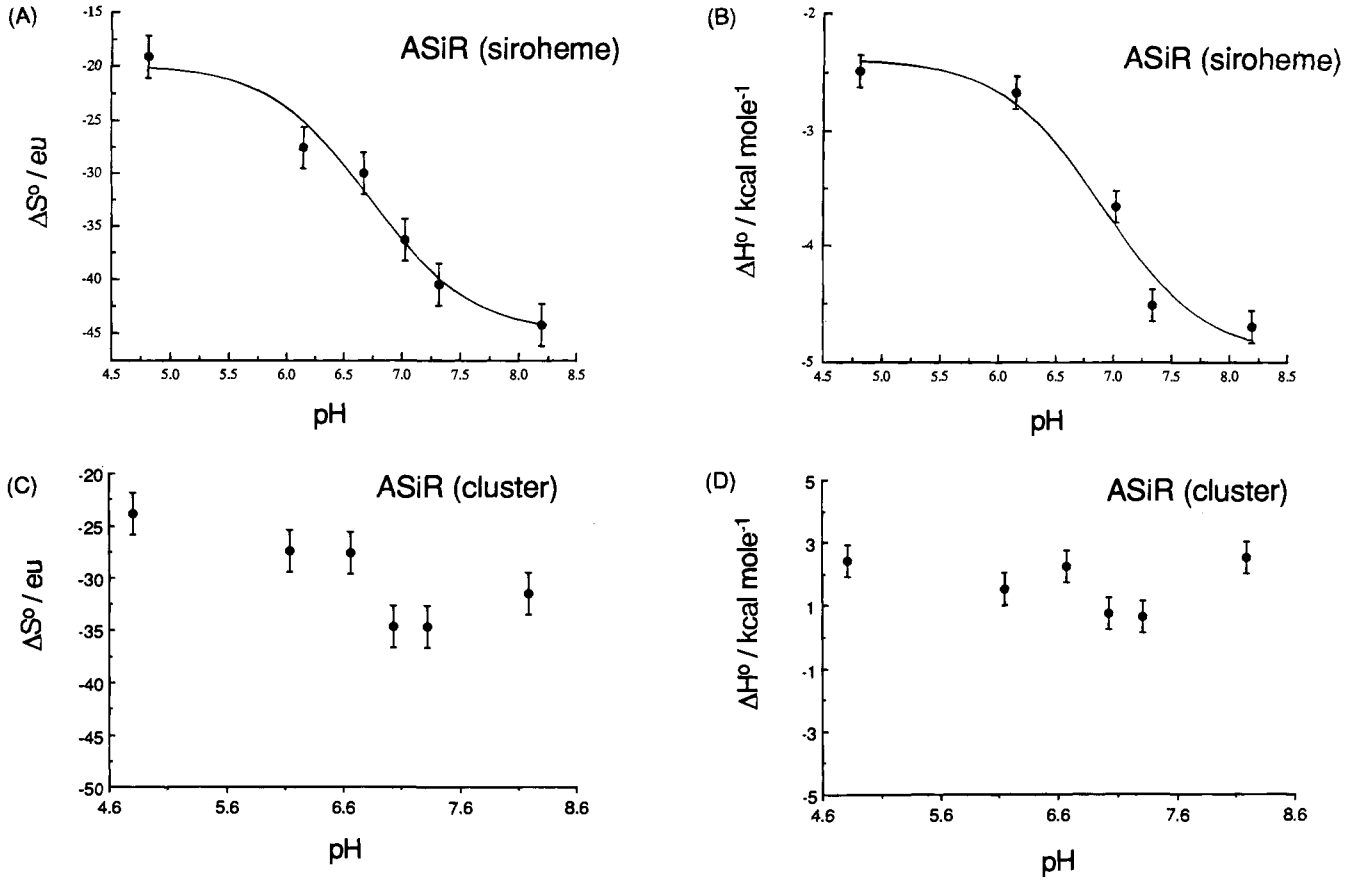

Figure 9. Plots of entropic and enthalpic components of siroheme and cluster redox couples *versus* pH for ASiR: (A) $\Delta S°$ *versus* pH for siroheme; (B) $\Delta H°$ *versus* pH for siroheme; (C) $\Delta S°$ *versus* pH for the $[Fe_4S_4]$ cluster; (D) $\Delta H°$ *versus* pH for the $[Fe_4S_4]$ cluster.

may arise from a more hydrophobic environment for siroheme inside the protein pocket. Inasmuch as there are no side-products produced during turnover of SO_3^{2-}, such as those observed for DSiR,[52] we have previously argued that the prosthetic center in ASiR is likely to be less solvent exposed or that entry to the active site shows a higher degree of steric hindrance.[53] Lower polarity (or a more hydrophobic environment) will lead to a more positive heme redox potential:[49] for example, the heme proteins Hb, Mb, and cyt *c* all have the redox active site (heme) buried inside a very hydrophobic medium. Finally, the less negative $E°'$ value for the heme center in ASiR may also reflect the smaller change in spin state upon reduction of the low-spin siroheme in this enzyme ($S = 1/2$ to $S = 0$) and the absence of significant change in electron configuration. A change of spin state upon reduction generally leads to more negative $E°'$ values, since this typically results in a significant redistribution of electrons over the d-orbital set that strongly influences metal–ligand geometries and promotes substantial activation barriers that impede reduction. There is evidence to support a change of spin state for *E. coli* sulfite reductase from high spin ($S = 5/2$) to an intermediate spin ($S = 1$) after one-electron reduction,[54] while oxidized DSiR also contains a high-spin siroheme ($S = 5/2$) and may also show a larger change of spin state and electronic configuration following reduction.

Reduction Potential of the Second Redox Couple. The Fe_4S_4 cluster in ASiR has a less negative $E°$ value (~ -300 mV) compared to the $E°$ value of the second redox couple in DSiR (-620 mV) and the Fe_4S_4 cluster in *E. coli* sulfite reductase (-405 mV).[55] This must reflect variations in the peptide environment surrounding the prosthetic centers in each enzyme. Perhaps most noteworthy is the rather negative (~ -620 mV) potential for the second redox couple of DSiR. This potential is not accessible with typical physiological reductants. We might expect that this potential would shift to less negative values after substrate (or ligand) binding following one-electron reduction. Experiments to test this hypothesis are a focus of current research effort in our laboratory.

General Comparison of Thermodynamic Parameters. Inasmuch as the enthalpies and entropies of metalloprotein electron-transfer processes are influenced by changes in protein conformation and solvation as well as by other structural and medium effects[21,23] comparison of these parameters with a series of well-defined redox proteins provides useful mechanistic insight on the factors regulating redox chemistry in this class of sulfite-reductase enzyme. In this, and subsequent sections we compare and contrast the thermodynamic parameters for electron exchange in ASiR, DSiR, Mb, and cyt *c* (Table 2). Values for myoglobin and cyt *c* are listed for comparison since Mb is pentacoordinate and cyt *c* is hexacoordinate, as are DSiR and ASiR, respectively. Also, Mb experiences a change in ligation sphere during reduction since an axial H_2O molecule is released and may serve as a point of reference for ASiR since there is likely to be a change in the coordination environment of siroheme during reduction arising from loss of the axial ligand; a prerequisite for substrate binding.

Surprisingly few reports of the temperature-dependence of

(52) (a) Postgate, J. R. *The Sulphate Reducing Bacteria*; Cambridge University Press: New York, 1984; p 86. (b) Seki, Y.; Ishimoto, M. *J. Biochem. (Tokyo)* **1981**, *90*, 1487–1492.

(53) Tan, J.; Cowan, J. A. *Biochemistry* **1991**, *30*, 8910–8917.

(54) (a) Christner, J. A.; Munck, E.; Janick, P. A.; Siegel, L. M. *J. Biol. Chem.* **1983**, *258*, 11147–11156. (b) Janick, P. A.; Siegel, L. M. *Biochemistry* **1982**, *21*, 3538.

(55) Siegel, L. M.; Rueger, D. C.; Barber, M. J.; Kruger, R. J.; Orme-Johnson, N. R.; Orme-Johnson, W. H. *J. Biol. Chem.* **1982**, *257*, 6343–6350.

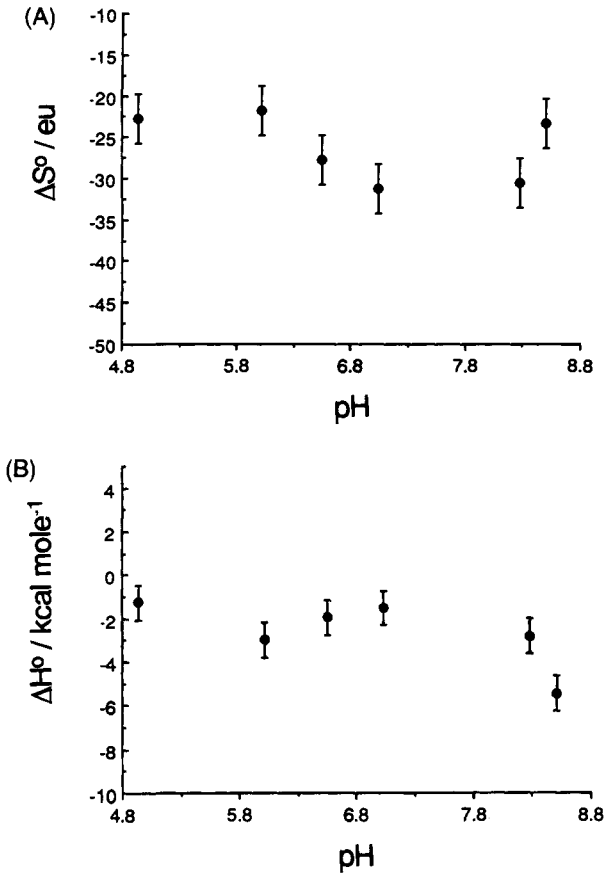

Figure 10. Plots of entropic and enthalpic components *versus* pH for the first redox couple of DSiR: (A) $\Delta S°$ *versus* pH and (B) $\Delta H°$ *versus* pH.

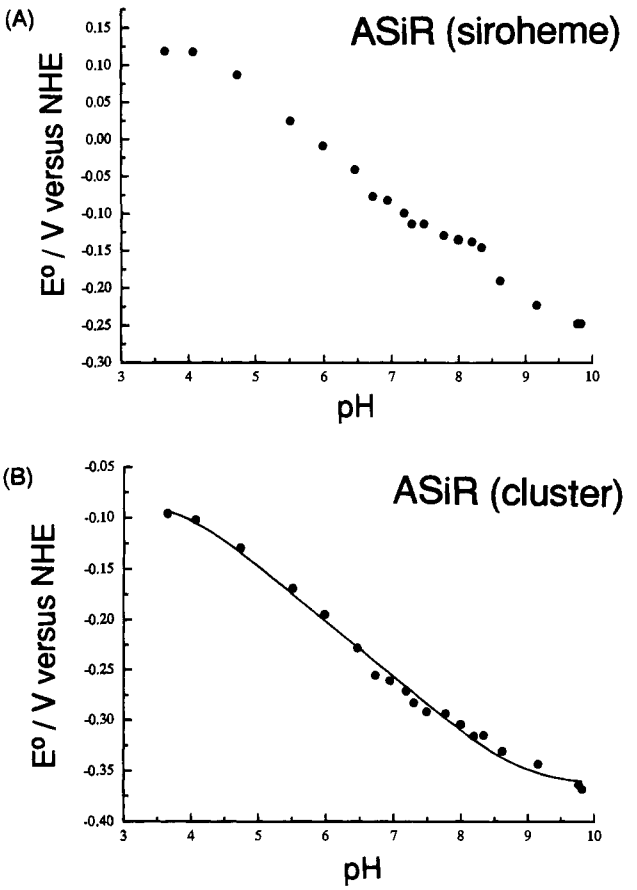

Figure 11. Variation of $E°$ (V) with pH for ASiR: (A) siroheme signal and (B) cluster signal. The data in (B) shows a fit to eq 4. The data in (A) does not show a fit to better indicate the deviation in the slope at pH ~7–8 that we ascribe to a siroheme-bound protein residue. Data were obtained from an 8 μM ASiR solution with 8 mM $Cr(NH_3)_6^{3+}$ in 10 mM potassium phosphate/10 mM NaCl under Ar(g) at 298 K. SWV conditions: pulse potential (E_p) = 50 mV; step potential (E_s) = 1 mV; frequency of the applied potential ν = 140 Hz.

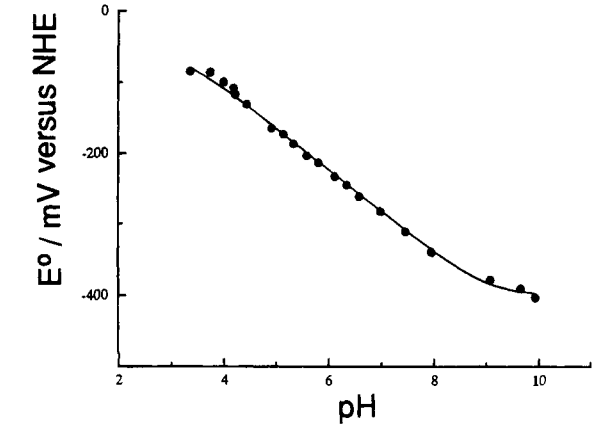

Figure 12. DSiR: variation of $E°$ (mV) with pH, showing a fit to eq 4 for the first redox couple (P^-). Data were obtained from a 10 μM DSiR solution with 8 mM $Cr(NH_3)_6^{3+}$ in 10 mM potassium phosphate/ 10 mM NaCl under Ar(g) at 298 K. SWV conditions: pulse potential, E_p = 50 mV; step potential, E_s = 1 mV; frequency of the applied potential, ν = 100 Hz.

[Fe_4S_4] cluster potentials have appeared in the literature. Those that do, tend to focus on high-potential iron proteins rather than low-potential ferredoxins.[22] Our results are therefore among the first to be reported for such centers. Inasmuch as the relevant pairs of oxidation states for high and low-potential ferredoxins are distinct, it is unclear whether the differences illustrated by the data in Table 2 between HiPIP and ASiR are significant. Clearly further characterization of redox parameters for low-potential ferredoxins would be of value.

Relative Magnitude and pH-Dependence of the $\Delta S°$ Values. The values of the entropy change $\Delta S°'$ (at pH 7.0 and 25 °C) are all negative in magnitude (Table 2), in contrast to typical results for transition-metal complexes which usually show a positive entropy change for positively-charged metal complexes and a negative entropy change for negatively-charged metal complexes.[21-24,56,57] Electrostatic charge factors and specific ligand solvation effects appear to dominate the entropy change exhibited by transition metal complexes.[35,56,57] Bulky and hydrophobic ligands (phenanthroline and bipyridine, for example) depress the magnitude of the observed $\Delta S°$. In contrast, metalloprotein redox couples tend to show negative entropy changes that do not correlate with protein charge.[21-24,58] The negative entropy change is most likely associated with structural change of the protein backbone and side-chains upon reduction. Previously it has been shown that Mb undergoes a change in inner sphere ligation upon reduction, with dissociation of an axial H_2O molecule and an accompanying large negative entropy change.[59,60] Significantly, the most negative entropy change is found with the low-spin assimilatory sulfite reductase.

(56) (a) Sutin, N.; Weaver, M. J.; Yee, E. L. *Inorg. Chem.* **1980**, *19*, 1096. (b) Marcus, R. A.; Sutin, N. *Inorg. Chem.* **1975**, *14*, 213.

(57) (a) Wawrousek, E. F.; McArdle, J. V. *J. Inorg. Biochem* **1982**, *17*, 169. (b) Tsou. Y.-M.; Anson, F. C. *J. Electrochem. Soc.* **1984**, *131*, 595. (c) Hupp, J. R.; Weaver, M. J. *J. Electrochem. Soc.* **1984**, *131*, 619. (d) Lieber, C. M.; Lewis, N. S. *J. Phys. Chem.* **1986**, *90*, 1002. (e) Schmitz, J. E. J.; van der Linden, J. G. M. *Inorg. Chem.* **1984**, *23*, 117. (f) Borchardt, D.; Wherland, S. *Inorg. Chem.* **1984**, *23*, 2537. (g) Borchardt, D.; Wherland, S. *Inorg. Chem.* **1982**, *21*, 93.

(58) Margalit, R.; Schejter, A. *FEBS Lett.* **1970**, *6*, 278.

Both the magnitude and pH-dependence of these data for ASiR are consistent with the presence of a labile axial ligand, and are in full accord with the distinct coordination of the low-spin siroheme in this enzyme relative to other members of the sulfite reductase family.[61] Figure 9A shows the variation of $\Delta S°$ with pH for the siroheme signal of ASiR. The sigmoidal curve gives a $pK_a^{ox} \sim 5.8$ and a $pK_a^{red} \sim 7.6$, which is most likely related to the dissociation of the axial ligand, possibly histidine as previously suggested on the basis of NMR data.[62] Clearly the magnitude of the negative $\Delta S°'$ in Table 2 shows no correlation with heme spin state.

Relative Magnitude and pH-Dependence of the $\Delta H°$ Values. It was noted that the siroheme in ASiR and the hemes in cyt *c* and Mb show a significantly more negative $\Delta H°'$ value (-11.8, −14.5, −14 kcal mol^{-1}, respectively, at pH 7.0 and 25 °C) in comparison to that determined for the ASiR cluster and the first redox couple of DSiR. The more negative $\Delta H°'$ values result from favorable d-π overlap between ferrous ion and heme/siroheme ligand. In contrast, $[Fe_4S_4]$ clusters typically show minimal change in Fe−S bonding and show the smaller negative $\Delta H°'$ values. The first redox couple for DSiR also has a smaller negative $\Delta H°'$ value; however, this may result in part from the significant cluster contribution to this redox couple (Figure 5).

Only the siroheme response from ASiR shows a demonstrable pH-dependence of $\Delta H°$ (Figure 9B), consistent with the pH-dependence of the entropic term (Figure 9A) and loss of an axial His ligand. Such observations are consistent with the requirement for ligand loss prior to substrate binding. It is interesting to speculate that such a protonated residue might serve to stabilize the bound substrate anion and/or facilitate proton transfer to oxygen during turnover. These issues are the topic of current investigation.

pH-Dependence of Reduction Potentials. The pH titration curves for the redox couples in DSiR and ASiR were found to have similar broad features. The ligand or residue affecting the change of $E°$ value with pH values is not a neighboring amino acid as the pH titration curve will not show such a broad feature. We postulated that this ligand must be directly bound to the redox center. In DSiR it can be either the bound H_2O at the sixth coordination site to the siroheme or the bridging S^{2-} ligand. If the pH behavior is due to the bound H_2O, it should not be observed in ASiR, which only possesses a protein-derived ligand at the axial site.[62] The redox centers in ASiR and DSiR show a similar broad pH dependence except for an additional feature with a $pK_a \sim 7-8$ buried under the broad pH titration curve of the siroheme signal of ASiR. This can be ascribed to an axial residue (most likely His), which has already been implicated in variable temperature experiments described earlier. The broad pH titration behavior is most likely due to a bridging sulfide that is directly bound to the redox centers in both ASiR and DSiR since there is no siroheme-bound H_2O in ASiR.

Although the discussion here has focussed extensively on the bridge site, it is questionable whether this site is actually protonated during active turnover, when it is more likely that the proton is captured by intermediate species formed by reduction of substrate. Our results do, however, demonstrate that a pathway exists which facilitates movement of protons from the bulk medium to the active site pocket and that this proton flux is indeed coupled to oxidation and reduction of the catalytic prosthetic centers. Indeed it is interesting to speculate that the movement of protons might be related in some way to the redox-linked conformational gating mechanism recently demonstrated for at least one member of this class of enzyme.[63] This connection remains to be established.

Coupling of the $[Fe_4S_4]$ Cluster and Siroheme. The generality of the coupled cluster−siroheme model for this class of enzyme has recently been questioned.[7] Previously published NMR data on ASiR supports direct coupling of the two redox centers,[62] following the original proposal of Siegel and co-workers for the *E. coli* enzyme.[14-16] The electrochemical data reported here for DSiR also provides strong support for a coupled prosthetic unit. In particular, the voltammetric response for the first redox couple (~298 mV *versus* NHE) encompasses both the siroheme and cluster redox centers. The redox potentials of each site remain similar over the pH range 3−10 (only one peak is observed), which would be unexpected if the two centers were uncoupled since one might expect that the similarity of $E°_{cluster}$ and $E°_{siroheme}$ would break down at some point over this large range if the centers were indeed uncoupled and dependent on their local environment to define the respective $E°$ values. In summary, these results support direct coupling of the siroheme and $[Fe_4S_4]$ cluster, forming a bridged redox pair (P) that apparently takes up two electrons in consecutive steps ($P \rightarrow P^- \rightarrow P^{2-}$) (Figure 6).

Concluding Remarks. The application of direct electrochemical methods to measure reduction potentials for $[Fe_4S_4]$−siroheme prosthetic centers in sulfite-reducing enzymes lays the groundwork for more detailed investigation of the redox chemistry of the coupled center common to this class. Characterization of the redox thermodynamics, pH-titration studies, and examination of catalytic reactions of these enzymes by direct electrochemical methods are now feasible.

Acknowledgment. We thank Don Ordaz for large-scale cultures of *D. vulgaris* and Richard McCreery and Mark Fryling for a generous gift of PGE and helpful discussions.

(59) (a) Takano, T. *J. Mol. Biol.* **1977**, *110*, 537. (b) Takano, T. *J. Mol. Biol.* **1977**, *110*, 569.

(60) Pauling, L. In *Hemoglobin*; Roughton, F. J. W., Kendrew, J. C., Eds.; Butterworth: London, 1949; p 57.

(61) Moura, I.; Lina, A. R.; Moura, J. J. G.; Xavier, A. V.; Fauque, G.; Peck, H. D.; LeGall, J. *Biochem. Biophys. Res. Commun.* **1986**, *141*, 1032−1041.

(62) Cowan, J. A.; Sola, M. *Inorg. Chem.* **1990**, *29*, 2176−2179.

(63) Lui, S. M.; Cowan, J. A. *Biochemistry* **1994**, *33*, 11209−11216.